Environ. Eng. Res. 2018; 23(4): 383-389
https://doi.org/10.4491/eer.2017.171

pISSN 1226-1025
eISSN 2005-968X

Improved structures of stainless steel current collector increase power generation of microbial fuel cells by decreasing cathodic charge transfer impedance

Taehui Nam[1], Sunghoon Son[1], Eojn Kim[1], Huong Viet Hoa Tran[1], Bonyoung Koo[1], Hyungwon Chai[1], Junhyuk Kim[1], Soumya Pandit[2], Anup Gurung[3], Sang-Eun Oh[3], Eun Jung Kim[4], Yonghoon Choi[5], Sokhee P. Jung[1†]

[1]*Department of Environment and Energy Engineering, Chonnam National University, Gwangju 61186, Republic of Korea*
[2]*The Zuckerberg Institute for Water Research, Ben-Gurion University of the Negev, Sede Boqer Campus, 8499000, Israel*
[3]*Department of Biological Environment, Kangwon National University, Chuncheon 24341, Republic of Korea*
[4]*Department of Environmental Engineering, Mokpo National University, Muan-gun 58554, Republic of Korea*
[5]*Department of Electrical Engineering, Chonnam National University, Gwangju 61186, Republic of Korea*

ABSTRACT

Microbial fuel cell (MFC) is an innovative environmental and energy system that converts organic wastewater into electrical energy. For practical implementation of MFC as a wastewater treatment process, a number of limitations need to be overcome. Improving cathodic performance is one of major challenges, and introduction of a current collector can be an easy and practical solution. In this study, three types of current collectors made of stainless steel (SS) were tested in a single-chamber cubic MFC. The three current collectors had different contact areas to the cathode (P 1.0 cm^2; PC 4.3 cm^2; PM 6.5 cm^2) and increasing the contacting area enhanced the power and current generations and coulombic and energy recoveries by mainly decreasing cathodic charge transfer impedance. Application of the SS mesh to the cathode (PM) improved maximum power density, optimum current density and maximum current density by 8.8%, 3.6% and 6.7%, respectively, comparing with P of no SS mesh. The SS mesh decreased cathodic polarization resistance by up to 16%, and cathodic charge transfer impedance by up to 39%, possibly because the SS mesh enhanced electron transport and oxygen reduction reaction. However, application of the SS mesh had little effect on ohmic impedance.

Keywords: Cathode, Current collector, Electrochemical impedance spectroscopy, Microbial fuel cells, Power density, Stainless steel

1. Introduction

Microbial fuel cell (MFC) is an innovative environmental and energy system that converts biomass energy in wastewater into electrical energy and purify wastewater by using microbial electrochemical reaction [1-5]. For the practical implementation of a MFC as a next generation wastewater treatment process, MFC performance should be enhanced far more than the current level [6, 7]. Significant advances have been made in improving MFC architecture, understanding the microbial community and their interaction and elucidating electrochemical reactions in last decades. However, in order to make MFC technology commercially feasible, a number of limitations need to be overcome. Among them, improving cathodic performance is one of the major challenges to the practical implementation [8]. For this reason, development of cathode technology with improved performance and low cost has been investigated a lot in the MFC field [9-13].

Nevertheless, it is necessary to improve the cathodic performance through valid strategies. In air cathodes, the catalytic layer

Received November 8, 2017 **Accepted** April 2, 2018

† Corresponding author
Email: sokheejung@chonnam.ac.kr, sokheejung@gmail.com
Tel: +82-62-530-1857 Fax: +82-62-530-1859
ORCID: 0000-0002-3566-5649

is in contact with sewage and oxygen reduction reaction (ORR) occurs when hydrogen ions, electrons and oxygen meet in the catalyst layer [14]. The power density produced by the MFC highly depends on the cathodic catalytic activity and the cathodic internal resistance [15, 16], which accounts for one of largest portion in determining MFC performance.

There have been a few cathode types so far in the MFC field [17]. The platinum-coated carbon cloth cathode is a most commonly used type, where tiny titanium wire is used as a current collector. This cathode produced up to 766 mW/m^2 of maximum power density in 50-mM PBS buffer and 5-mM acetate [18]. Most recently, the stainless-steel-based cathode coated with activated carbon catalyst has been developed, which produces up to 802 mW/m^2 in 50 mM PBS buffer and 10 mM acetate [19]. Recent research shows that activated-carbon based cathodes produced more power than platinum-based cathodes in MFC. Since platinum is known to have a better catalytic activity, these results imply that the metal cathodic base in activated-carbon cathode facilitate electron flow in this cathode.

Metallic current collector is used as inexpensive current collectors for anodes and cathodes in MFCs. For example, a metallic core rod of a carbon fiber brush is used to promote electron transfer from the bacteria to the external circuit, which produced a maximum power density of 2,400 mW/m^2 in lab scale reactors [20]. The stainless steel (SS) mesh has been used as a cathode base, replacing carbon cloth [9, 10, 21]. The addition of SS mesh to the surface of an anion exchange membrane coated with a conductive graphite paint increased maximum power density from 450 mW/m^2 to 575 mW/m^2 [10]. These results suggest that introduction of current collector to the cathode electrode can improve the performance of the MFC.

The surface area of the current collector could affect the electron transport in the cathode. However, there is little report available regarding the influence of the current collector area of cathode on MFC performance. Therefore, in this study, it is hypothesized that increasing area of the current collector attached on the cathode electrode could increase electron transfer rate and power generation. To confirm this hypothesis, three current collectors having different surface areas were tested in a single-chamber cubic MFC with a carbon fiber brush anode and a Pt-coated carbon cloth cathode. As a metal current collector material, non-corrosive stainless steel (SUS 304) was applied. We found that increasing current collector of the cathode enhance MFC performance.

2. Materials and Methods

2.1. MFC Construction

A platinum-coated carbon-cloth cathode was made of carbon cloth (surface area 7 cm^2; 30% wet proofing; AvCarb 1071 HCB, Fuel cell earth, Boston, U.S.A.), with a PTFE diffusion layer on the air facing side (60wt% dispersion in H_2O, Sigma-Aldrich, Young-in, Korea) and a Pt catalyst layer (0.5 mg/cm^2, 10% Pt on carbon, Sigma-Aldrich, Young-in, Korea) on the solution side [22]. Three different current collectors were made of non-corrosive stainless steel plate (SUS 304) and stainless steel mesh (# 30, type SUS 304). A broad stainless steel plate (1 cm^2 of contact area) (P), a broad stainless steel plate with a rounded-rim (4.3 cm^2 of contact area) (PC), and a broad stainless steel plate with a stainless steel mesh (# 30, type SUS 304) (6.5 cm^2 of contact area) (PM) were applied to a Pt-coated carbon cloth cathode (Fig. 1) [9, 23].

A single-chamber cubic-shaped reactor was made with polycarbonate, having 28 mL cylindrical bed volume of 4-cm length

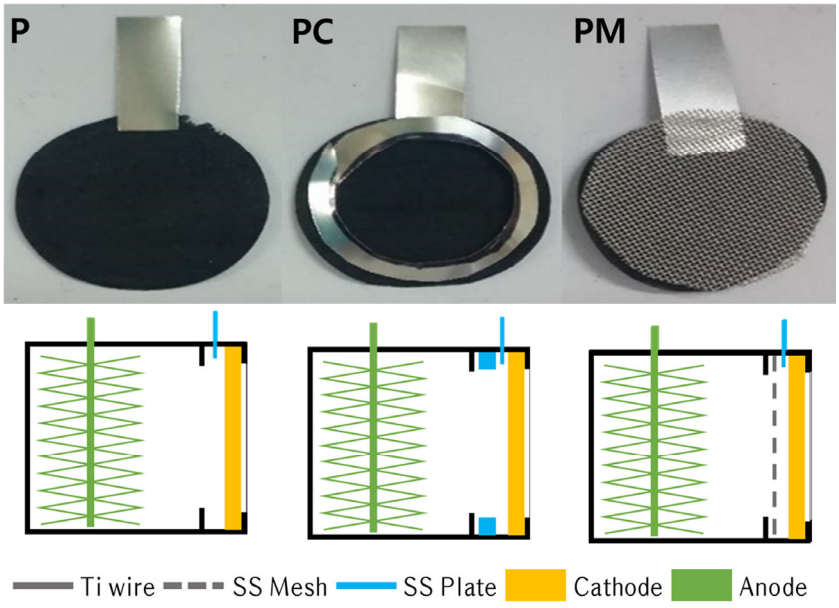

Fig. 1. The cathodes with three different current collectors and their schematics in the MFC. A stainless steel plate was used as an electrode connector (1.0 cm^2 of contact area) (P), a stainless steel plate and a rounded-rim current collector were used (4.3 cm^2 of contact area) (PC), and a stainless steel plate and a stainless-steel-mesh current collector were used (6.5 cm^2 of contact area) (PM).

and 3-cm diameter [21, 24-26]. A brush electrode was made with a carbon fiber brush (25-mm diameter and 50-mm length) twisted between two titanium rods (length 70 mm, 17 gauge; grade 2, Seoul Titanium). It was heat-treated at 450°C for 30 min in a normal atmosphere condition [27] and located in the reactor horizontally to the cathode without a separator as previously described [25].

2.2. Inoculation and Operation

The MFC was inoculated with 28 mL of domestic wastewater (Gwangju Wastewater Treatment Plant) and was operated with 1,000-Ω external resistance in a fed-batch mode. When the voltage started to exceed 100 mV, the internal solution was replaced with the 50-mM PBS medium (CH_3COONa 0.41 g/L, NaH_2PO_4 2.34 g/L, Na_2HPO_4 4.33 g/L, NH_4Cl 0.31 g/L, KCl 0.13 g/L, trace mineral solution 10 mL/L and vitamin solution 10 mL/L) [28, 29]. Medium was replaced when the voltage decreased to less than 10 mV. During the MFC operation, its voltage was measured using a systems switch/multimeter (3706A, Keithley).

2.3. Electrochemical Tests

Three cathode current collectors (P, PC, and PM) were tested under the same medium conditions with the same brush anode in order to minimize experimental variation [30]. All experiments were conducted in the MFC system, except for a current collector. Electrochemical analysis was performed using a potentiostat (ZIVE SP1, Wonatech, Korea). For electrochemical measurement, a Ag/AgCl reference electrode (RE-1B, ALS, Japan; -0.209 V vs. SHE) was inserted in the medium through a rubber gasket and located in the middle of the MFC.

For polarization tests, the MFC was operated at 1,000-Ω external resistance for 3 h after medium change. Then, it was sit in an open circuit mode in a potentiostat for 2 h, followed by an electrochemical experiment. Electrical leads of the MFC was connected to a potentiostat as follows: a cathode to a working lead, an anode to a counter lead, a reference lead and an AI+ lead, a reference electrode to an AI- lead. Polarization curves were recorded through the linear sweep voltammetry (LSV) technique by decreasing cell voltage from OCV to 0 with a scan rate of 1 mV/s. Polarization measurement was performed in duplicate.

Power density (p, mW/m^2) was calculated using the following equations:

$$p = \frac{I \times V}{A} \quad (1)$$

$$\frac{I}{A} = i \quad (2)$$

where I is current (mA), V is voltage (mV), A is a projected cathode area (7 cm^2) and i is current density (mA/m^2) [31].

Polarization resistances of anode (R_{an}), cathode (R_{cat}) and full cell (R_{int}) were calculated from a slope of linear part of each polarization curve.

Optimum external resistance was calculated as following:

$$R_{opt} = \frac{V_{opt}}{I_{opt}} = \frac{P_{max}}{{I_{opt}}^2} \quad (3)$$

where R_{opt} is optimal external resistance for maximum power generation, V_{opt} is the optimum cell voltage for maximum power generation, A is the projected cathode area, P_{max} is maximum power and I_{opt} is optimal current for maximum power generation.

Electrochemical impedance spectroscopy (EIS) for cathode electrodes was carried out in a three-electrode configuration. After medium change, the MFC was operated at 1,000 Ω external resistance for 3 h. Then, the MFC was connected to a potentiostat as described above, held in an open circuit mode for 5 min, and operated at an optimum current in a galvanostatic mode for 20 min. Cathode impedance was measured at an optimum current for each cathode, where maximum power is produced. 0.1 mA of the amplitude of the alternating current and 10^5 - 10^{-2} Hz of the frequency range were used for cathodic impedance measurement.

2.4. Calculation

Coulombic efficiencies (CE) were calculated as the ratio of recovered coulombs to the theoretical amount of coulombs that could be produced from organic matter oxidation based on the change of total COD [6]. In order to measure the COD, the external resistance of the reactor was connected to 1,000 Ω. For total COD measurements, the medium of the reactor was replaced, the reactor was shaken and a sample was immediately taken. For soluble COD measurements, samples were taken when the voltage was below 50 mV and filtered through syringe filters (pore size 0.45 μm, 13 mm diameter, PVDF, CT-K Corporation). CE was calculated by the following equation:

$$CE = \frac{\int_0^t Idt}{F\,V\,\triangle COD/8} \times 100 \quad (4)$$

where F is Faraday's constant (96,485.3329 C/e-mol), V is the bed volume of the MFC (0.028 L), ΔCOD is the change in COD during operation time (g-COD) and 8 is a conversion factor (8 g-COD/e-mol). COD measurements were performed using a portable spectrophotometer (X-100, C-MAC, Daejeon, Korea). Final CODs were measured by using medium samples when the MFC voltage 50 mV.

Energy efficiency (EE) was calculated by the following equation:

$$EE = \frac{\int_0^t VIdt}{\triangle Hn} \times 100 \quad (5)$$

where ΔH is the heat of combustion of acetic acid (-875 kJ/mol) and n is the amount (mol) of substrate consumed.

All the potential values in this manuscript were reported in the SHE scale by using the following equation:

$$\text{mV vs. SHE} = \text{mV vs. Ag/AgCl} + 209\ \text{mV} \quad (6)$$

3. Results

3.1. Power Density Curves and Polarization Curves

A stainless steel plate (P), a stainless steel plate with a rounded-rim (PC), and a stainless steel plate with a stainless steel mesh (PM) were applied to a Pt-coated carbon cloth cathode, and three different cathodes were tested in the MFC. Contacting area of a carbon cloth cathode to a metal current collector was largest in the PM cathode (6.5 cm^2), followed by the PC cathode (4.3 cm^2), the P cathode (1.0 cm^2) (Fig. 1). As contacting area of a carbon cloth cathode to a metal current collector increased, MFC performance also increased in the order of PM, PC and P.

Among three different current collectors, PM produced the highest maximum power density (1,136 mW/m^2), followed by PC (1,061 mW/m^2) and P (1,044 mW/m^2) in average (Fig. 2(a), Table 1). PM also produced the highest optimum current density (3,752 mA/m^2), followed by PC (3,715 mA/m^2), P (3,621 mA/m^2) in average. PM produced the highest maximum current density (7,610 mA/m^2), followed by PC (7,346 mA/m^2), P (7,133 mA/m^2). Application of a stainless steel mesh to the cathode (PM) improved maximum power density, optimum current density and maximum current density of the MFC by 8.8%, 3.6% and 6.7%, respectively, comparing with P having no stainless steel mesh.

Polarization resistance obtained from a linear part of each polarization curve in duplicate and their average was calculated (Fig. 2, Table 1) [32]. PM had the lowest cathodic polarization resistance (81 Ω), followed by PC (84 Ω), P (96 Ω). For anodic polarization resistance, P had the lowest value (30 Ω), followed by PM (43 Ω), PC (44 Ω). Cathodic polarization esistance was higher than anodic polarization resistance by 47% in P, 48% in PC, and 69% in P. Internal resistances were 123 Ω for P, 122 Ω for PC and 121 Ω for PM. Maximum power density can be produced when MFC is operated at an optimum external resistance, and they were 113 Ω for P, 109 Ω for PC and 105 Ω for PM. Optimum external resistance values were pretty similar to internal resistance values. Activation loss is detected in a low current region of in cathode polarization curves (Fig. 2(b)), showing activation loss were originated mainly from the cathode.

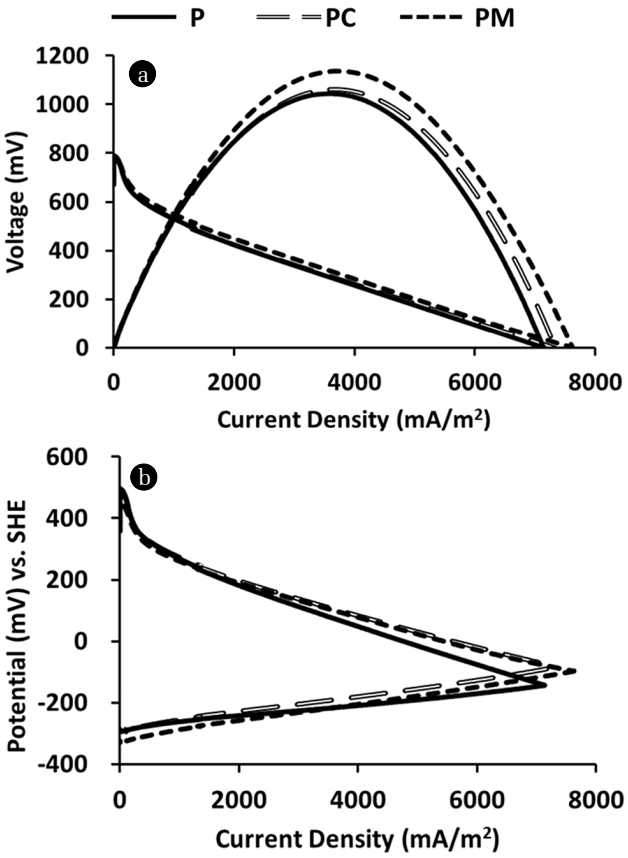

Fig. 2. Polarization and power density curves of full cells (a), and polarization curves of anode and cathode electrodes (b).

3.2. Electrochemical Impedance Spectroscopy Analysis

For more accurate and delicate measurement of ohmic and charge transfer impedance of the cathodes by excluding other irrelevant factors, cathodic EIS was performed in a galvanostatic mode at each optimum current for each MFC condition (Fig. 3 and Fig. 4). PM, producing the highest maximum power density, showed lowest cathodic ohmic and charge transfer impedance. Cathodic ohmic impedances were slightly different in the three

Table 1. Analytical Data of Polarization and Power Density Curves (n = 2), Electrode Potentials Were Written in the SHE Scale

	OCV (mV)	p_{max} (mW/m^2)	i_{max} (mA/m^2)	i_{opt} (mA/m^2)	R_{opt} (Ω)
P	757 ± 8	1,044 ± 184	7,133 ± 786	3,621 ± 462	113 ± 10
PC	762 ± 3	1,061 ± 155	7,346 ± 861	3,715 ± 424	109 ± 8
PM	772 ± 8	1,136 ± 104	7,610 ± 973	3,752 ± 430	115 ± 14
	E_{an}^{opt} (mV)	E_{cat}^{opt} (mV)	R_{int} (Ω)	R_{cat} (Ω)	R_{an} (Ω)
P	-208.7 ± 13	61.8 ± 10	123 ± 8	96 ± 2	30 ± 9
PC	-192.3 ± 8	79.2 ± 17	122 ± 10	84 ± 1	44 ± 11
PM	-205.3 ± 9	81.1 ± 14	121 ± 15	81 ± 7	43 ± 9

OCV, open circuit voltage; p_{max}, maximum power density; i_{max}, maximum current density; i_{opt}, optimal current density; R_{opt}, optimal external resistance; E_{an}^{opt}, optimum anode potential; E_{cat}^{op}, optimum cathode potential; R_{int}, internal resistance of a full cell; R_{cat}, cathodic polarization resistance; R_{an}, anodic polarization resistance

forms. PM had the lowest ohmic impedance (20 Ω) followed by PC (21 Ω) and P (22 Ω). However, there was bigger difference in cathodic charge transfer impedance. PM also had the lowest cathodic charge transfer resistance (53 Ω), followed by PC (72 Ω), P (97 Ω). Cathodic charge transfer impedance of PM was 54% lower than that of P.

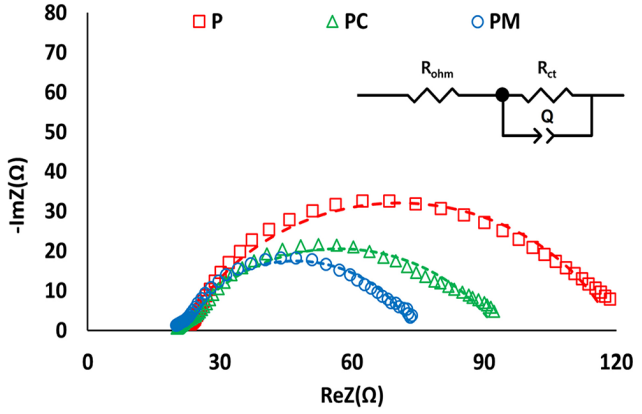

Fig. 3. Nyquist plots and the equivalent circuit fittings of the cathodic EIS (dotted line) at the optimum current. The inset is the equivalent circuit for fitting cathode EIS: R_{ohm} is ohmic impedance, R_{ct} is charge transfer impedance, Q is constant phase element (CPE).

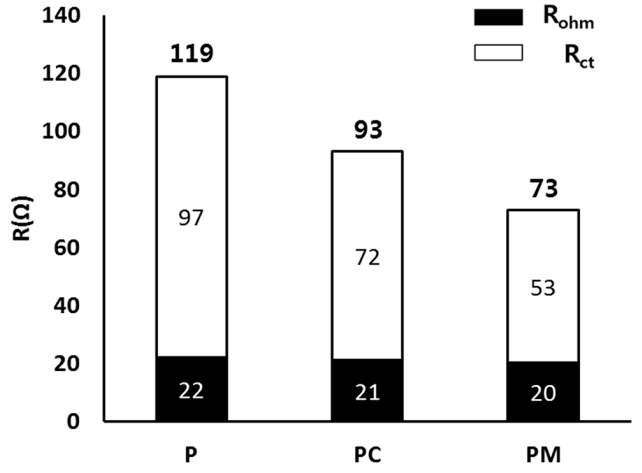

Fig. 4. Ohmic impedance (R_{ohm}) and charge transfer impedance (R_{ct}) in cathodes with different current collectors. A galvanostatic cathode EIS was performed at each optimum current in each cathode. Optimum current for cathodic EIS was 2.0 mA for P, 2.1 mA for PC and 2.3 mA for PM (n = 1).

3.3. COD Removal, Coulombic Efficiency and Energy Efficiency

PC showed the highest CE (19.8%), followed by PM (19.0%) and P (15.0%). PC also showed the highest EE (6.4%), followed by PM (5.7%) and P (4.6%) (Table 2). These results show that introducing current collector on cathode enhances coulombic and energy recovery.

4. Discussion

Increasing contacting area of a carbon cloth cathode to a metal current collector increased the power and current densities of the MFC by decreasing cathodic resistance. Among the three cathodic current collectors, a combination of stainless plate and a stainless steel mesh (PM) was the best current collector design for maximizing MFC performance.

Due to the low electrical conductivity of the carbon cloth, carbon cloth cathode combined with a combination of stainless plate and a stainless steel mesh can be a practical solution for increasing power production. As a current collector, the stainless steel plate has a larger area than the conventional titanium wire, so that electrons from the bioanode can be supplied to the cathode with a less electrical resistance. In addition, the stainless steel mesh covers the entire carbon cloth cathode, so that it can directly supply electrons to the cathodic catalyst. Therefore, total cathodic resistance was reduced in this study.

By applying a stainless steel mesh (SSM), cathodic polarization resistance decreased by up to 16%, and cathodic charge transfer impedance decreased by up to 39%, comparing with the P. Ohmic resistance includes contact resistance in the electrode, electrode material resistance and solution resistance. Charge transfer resistance has to do with the process of electron transfer from one phase (e.g. electrode) to another (e.g. liquid). In the cathode system in our study, cathodic oxygen reduction is the main source of cathodic charge transfer resistance. Cathodic ohmic impedances of the three cathodes were very similar, showing that current collector did not influence contact resistance and material resistance in the cathodes so much in this study. However, the application of current collectors decreased charge transfer resistance significantly, implying that the SSM enhanced oxygen reduction reaction on the surface of the SSM. Previous studies also demonstrated use of stainless steel as cathode material for oxygen reduction [33-35].

The PM produced only 6.6% higher maximum power than the PC mainly by decreasing the charge transfer impedance by 25.8%. The area covered by a current collector over the platinum

Table 2. CE, EE, COD Removal Ratio, and Initial and Final CODs for Each Cathodic Condition. When MFC Voltage Decreased to Less Than 10 mV, MFC Operation Was Stopped and Medium Was Replaced

	CE (%)	EE (%)	Initial COD (mg/L)	Final COD (mg/L)	COD removal rate (mg/L·h)	Batch time (h)	COD removal ratio (%)
P	15.0	4.6	320	33.0	10.1	28.5	89.6
PC	19.8	6.4	320	17.6	15.1	20.0	94.5
PM	19.0	5.7	320	14.6	13.3	23.0	95.4

layer was larger in the PM (6.5 cm^2) than in the PC (4.3 cm^2), these might interfere with mass transfer and cathodic reduction. However, both platinum and SSM can perform an oxygen reduction reaction. Because stainless steel has less oxygen reduction performance than platinum, there was not the big difference in maximum power production between the PM and the PC despite the difference in the current collector coverage.

In our study, the applied currents for EIS were different among the tested MFCs. Their charge transfer resistance difference might be due to their different applied currents. According to a previous study, anodic charge transfer impedance decreased as current density increased, but cathodic charge transfer impedance was almost unaffected by applied potential or current for EIS [36]. Therefore, the change in charge transfer resistance among the MFCs might be attributed to the different cathode structures rather than the applied currents for EIS.

One of main concerns in the scale-up of MFC is significant decrease of power density as electrode size increases [37]. Introducing SSM may resolve this problem in large-area cathodes by facilitating electron transfer and reducing cathodic charge transfer resistance. Since high hydrostatic pressure is another concern in practical implementation of MFC, a durable and rigid cathode for hydrostatic pressure is necessary. The SSM can give high mechanical strength to the cathode electrode, so that it can help the cathode electrode with withstanding the high pressure.

Activation loss is the voltage loss that occurs when an electrochemical reaction is initiated. In the present study, cathodic activation loss was the main activation loss in the MFC (Fig. 2), showing that abiotic catalyst in cathode is the main source of activation loss rather than the anodic microbial catalyst. This result is coincident with the previous observation of negligible activation loss in the bioanode [36].

5. Conclusions

Increasing contacting area of a carbon cloth cathode to a metal current collector increased the power, current densities, and coulombic and energy recovery of the MFC by decreasing cathodic resistance. Among three different current collectors, the PM cathode with a SS plate and a SS mesh produced the highest maximum power (1,136 mW/m^2), the highest optimum current (3,752 mA/m^2) and the highest maximum current (7,610 mA/m^2). Application of a SS mesh to the cathode (PM) improved maximum power density, optimum current density and maximum current density of the MFC by 8.8%, 3.6% and 6.7%, respectively, comparing with P having no SS mesh. PM had the lowest cathodic polarization resistance (81 Ω), followed by PC (84 Ω), P (96 Ω). Internal resistances were 123 Ω for P, 122 Ω for PC and 121 Ω for PM. Cathodic polarization resistance was 47% higher in P, 48% higher in PC and 69% higher in P than anodic polarization resistance. Cathodic ohmic impedances were slightly different in the three forms: 20 Ω for PM, 21 Ω for PC and 22 Ω for P. However, there was bigger difference in cathodic charge transfer impedance: 53 Ω for PM, 72 Ω for PC and 97 Ω for P. In overall, by applying a SSM, cathodic polarization resistance decreased by up to 16%, and cathodic charge transfer impedance decreased by up to 39%. These enhancements in PM are possibly due to a SSM facilitating efficient electron transport and effective oxygen reduction reaction on the surface of the SSM. Application of a current collector decreased charge transfer resistance significantly, but affected ohmic resistance negligibly. PC showed the highest CE (19.8%) and EE (6.4%), followed by PM (CE 19.0% and EE 5.7%) and P (CE 15.0% and EE 4.6%). Cathodic activation loss was the main activation loss in the MFC.

Acknowledgments

This research was supported by Basic Science Research Program through the National Research Foundation of Korea (NRF) funded by the Ministry of Science, ICT & Future Planning (NRF-2015R1C1A1A02037493) and a research grant from Gwangju Green Environment Center in Ministry of Environment (17-04-10-14-12).

This article contains contents of the master thesis of Taehui Nam in 2017. This article also contains contents presented in a few academic conferences: 2016 Korean Water Congress, 2016 KSBB Spring Meeting and International Symposium, 2016 KSIEC Spring Meeting, 2016 AP-ISMET conference, 2016 ABBS and 2016 Korean Society of Environmental Engineers Conference. The authors certify that there is no authorship dispute among the authors.

References

1. Logan BE. Peer reviewed: Extracting hydrogen and electricity from renewable resources. *Environ. Sci. Technol.* 2004;38:160A-167A.
2. Lovley DR. Bug juice: Harvesting electricity with microorganisms. *Nat. Rev. Microbiol.* 2006;4:497-508.
3. Rabaey K, Verstraete W. Microbial fuel cells: Novel biotechnology for energy generation. *Trends Biotechnol.* 2005;23:291-298.
4. Jung SP. Practical implementation of microbial fuel cells for bioelectrochemical wastewater treatment. *J. Korean Soc. Urban Environ.* 2013;13:93-100.
5. Lee T, Okamoto A, Jung S, et al. Microbial electrochemical technologies producing electricity and valuable chemicals from biodegradation of waste organic matters. In: Yates M NC, Miller R, Pillai S, eds. Manual of environmental microbiology. 4th ed. American Society of Microbiology; 2016. p. 5.1.4-1-5.1.4-14.
6. Logan BE, Hamelers B, Rozendal R, et al. Microbial fuel cells: Methodology and technology. *Environm. Sci. Technol.* 2006;40:5181-5192.
7. Logan BE, Regan JM. Microbial fuel cells-challenges and applications. *Environ. Sci. Technol.* 2006;40:5172-5180.
8. Oh S, Min B, Logan BE. Cathode performance as a factor

in electricity generation in microbial fuel cells. *Environ. Sci. Technol.* 2004;38:4900-4904.
9. Zhang F, Saito T, Cheng S, Hickner MA, Logan BE. Microbial fuel cell cathodes with poly (dimethylsiloxane) diffusion layers constructed around stainless steel mesh current collectors. *Environ. Sci. Technol.* 2010;44:1490-1495.
10. Zuo Y, Cheng S, Logan BE. Ion exchange membrane cathodes for scalable microbial fuel cells. *Environ. Sci. Technol.* 2008;42:6967-6972.
11. Zhang F, Merrill MD, Tokash JC, et al. Mesh optimization for microbial fuel cell cathodes constructed around stainless steel mesh current collectors. *J. Power Sources* 2011;196: 1097-1102.
12. Dong H, Yu H, Wang X. Catalysis kinetics and porous analysis of rolling activated carbon-PTFE air-cathode in microbial fuel cells. *Environ. Sci. Technol*. 2012;46:13009-13015.
13. Wang X, Feng C, Ding N, et al. Accelerated OH^- transport in activated carbon air cathode by modification of quaternary ammonium for microbial fuel cells. *Environ. Sci. Technol*. 2014;48:4191-4198.
14. Liu H, Ramnarayanan R, Logan BE. Production of electricity during wastewater treatment using a single chamber microbial fuel cell. *Environ. Sci. Technol*. 2004;38:2281-2285.
15. Cheng S, Liu H, Logan BE. Power densities using different cathode catalysts (Pt and CoTMPP) and polymer binders (Nafion and PTFE) in single chamber microbial fuel cells. *Environ. Sci. Technol*. 2006;40:364-369.
16. Kim BH, Chang IS, Gadd GM. Challenges in microbial fuel cell development and operation. *Appl. Microbiol. Biotechnol.* 2007;76:485-494.
17. Yuan H, Hou Y, Abu-Reesh IM, Chen J, He Z. Oxygen reduction reaction catalysts used in microbial fuel cells for energy-efficient wastewater treatment: A review. *Mater. Horiz.* 2016;3:382-401.
18. Cheng S, Liu H, Logan BE. Increased performance of single-chamber microbial fuel cells using an improved cathode structure. *Electrochem. Commun*. 2006;8:489-494.
19. Dong H, Yu H, Wang X, Zhou Q, Feng J. A novel structure of scalable air-cathode without Nafion and Pt by rolling activated carbon and PTFE as catalyst layer in microbial fuel cells. *Water Res.* 2012;46:5777-5787.
20. Logan B, Cheng S, Watson V, Estadt G. Graphite fiber brush anodes for increased power production in air-cathode microbial fuel cells. *Environ. Sci. Technol.* 2007;41:3341-3346.
21. Koo B, Kang H, Nam T, Kim E, Son S, Jung SP. Performance enhancement of a microbial fuel cell by physico-chemical treatments of activated-carbon catalyst of an air cathode. *J. Korean Soc. Urban Environ.* 2016;16:431-439.
22. Middaugh J, Cheng S, Liu W, Wagner R. How to make cathodes with a diffusion layer for single-chamber microbial fuel cells. 2006.
23. Escapa A, San-Martín M, Mateos R, Morán A. Scaling-up of membraneless microbial electrolysis cells (MECs) for domestic wastewater treatment: Bottlenecks and limitations. *Bioresour. Technol.* 2015;180:72-78.
24. Liu H, Logan BE. Electricity generation using an air-cathode single chamber microbial fuel cell in the presence and absence of a proton exchange membrane. *Environ. Sci. Technol.* 2004;38:4040-4046.
25. Kang H, Jeong J, Gupta PL, Jung SP. Effects of brush-anode configurations on performance and electrochemistry of microbial fuel cells. *Int. J. Hydrogen Energ.* 2017;42:27693-27700.
26. Nam T, Son S, Koo B, et al. Comparative evaluation of performance and electrochemistry of microbial fuel cells with different anode structures and materials. *Int. J. Hydrogen Energ.* 2017;42:27677-27684.
27. Feng Y, Yang Q, Wang X, Logan BE. Treatment of carbon fiber brush anodes for improving power generation in air-cathode microbial fuel cells. *J. Power Sources* 2010;195: 1841-1844.
28. Jung S. Impedance analysis of *Geobacter sulfurreducens* PCA, *Shewanella oneidensis* MR-1, and their coculture in bioeletrochemical systems. *Int. J. Electrochem. Sci.* 2012;7: 11091-11100.
29. Jung S, Mench MM, Regan JM. Impedance characteristics and polarization behavior of a microbial fuel cell in response to short-term changes in medium pH. *Environ. Sci. Technol.* 2011;45:9069-9074.
30. Jung S, Regan JM. Comparison of anode bacterial communities and performance in microbial fuel cells with different electron donors. *Appl. Microbiol. Biotechnol.* 2007;77:393-402.
31. Aelterman P, Rabaey K, Pham HT, Boon N, Verstraete W. Continuous electricity generation at high voltages and currents using stacked microbial fuel cells. *Environ. Sci. Technol.* 2006;40:3388-3394.
32. Fan Y, Sharbrough E, Liu H. Quantification of the internal resistance distribution of microbial fuel cells. *Environ. Sci. Technol.* 2008;42:8101-8107.
33. Le Bozec N, Compère C, L'Her M, Laouenan A, Costa D, Marcus P. Influence of stainless steel surface treatment on the oxygen reduction reaction in seawater. *Corros. Sci.* 2001;43:765-786.
34. Kim YP, Fregonese M, Mazille H, Feron D, Santarini G. Study of oxygen reduction on stainless steel surfaces and its contribution to acoustic emission recorded during corrosion processes. *Corros. Sci.* 2006;48:3945-3959.
35. Dumas C, Mollica A, Feron D, Basseguy R, Etcheverry L, Bergel A. Marine microbial fuel cell: Use of stainless steel electrodes as anode and cathode materials. *Electrochim. Acta.* 2007;53:468-473.
36. Jung S, Oh S-E, Lee J, et al. Impedance and thermodynamic analysis of bioanode, abiotic anode, and riboflavin-amended anode in microbial fuel cells. *Bull. Korean Chem. Soc.* 2012;33:3349-3354.
37. Logan BE, Wallack MJ, Kim K-Y, He W, Feng Y, Saikaly PE. Assessment of microbial fuel cell configurations and power densities. *Environ. Sci. Technol. Lett.* 2015;2:206-214.